

Application of magnetohydrodynamic actuation to continuous flow chemistry†

Jonathan West,^{*a} Boris Karamata,^a Brian Lillis,^a James P. Gleeson,^b John Alderman,^a John K. Collins,^c William Lane,^a Alan Mathewson^a and Helen Berney^a

^a National Microelectronics Research Centre (NMRC), Cork, Ireland. E-mail: jwest@nmrc.ie;

Fax: +353 21 4270271

^b NMRC and Department of Applied Mathematics, UCC, Cork, Ireland

^c Department of Microbiology, UCC, Cork, Ireland

Received 11th July 2002, Accepted 12th August 2002

First published as an Advance Article on the web 22nd August 2002

Continuous flow microreactors with an annular microchannel for cyclical chemical reactions were fabricated by either bulk micromachining in silicon or by rapid prototyping using EPON SU-8. Fluid propulsion in these unusual microchannels was achieved using AC magnetohydrodynamic (MHD) actuation. This integrated micropumping mechanism obviates the use of moving parts by acting locally on the electrolyte, exploiting its inherent conductive nature. Both silicon and SU-8 microreactors were capable of MHD actuation, attaining fluid velocities of the order of $300 \mu\text{m s}^{-1}$ when using a 500 mM KCl electrolyte. The polymerase chain reaction (PCR), a thermocycling process, was chosen as an illustrative example of a cyclical chemistry. Accordingly, temperature zones were provided to enable a thermal cycle during each revolution. With this approach, fluid velocity determines cycle duration. Here, we report device fabrication and performance, a model to accurately describe fluid circulation by MHD actuation, and compatibility issues relating to this approach to chemistry.

1. Introduction

The ability to perform chemistries in microfabricated chambers presents many benefits that include reduced reagent volumes for safety and economy, and improved performance from increased thermal and mass transfer. Combining these benefits with modifications to achieve microchannels, and the provision of pumps for fluidic actuation enables new functionality and the possibility for an alternative approach to chemistry. Here, reactants flow through a spatially defined environment that permits the precise control and selectivity of chemical interactions for the synthesis of desired products.

Conducting chemistry with microfluidics has numerous attractive attributes. When actuating fluid in channels with micron dimensions laminar flow behaviour typically dominates. Fast, diffusion limited processes can benefit from appropriate channel arrangements for the generation of co-current laminar streams to provide high surface area to volume ratios for micromixing.^{1,2} This principle has been exploited for phase transfer reactions, including direct fluorination and nitration of organic compounds^{3,4} and separations.⁵ Flow through a micro-fabricated environment also confers the possibility to regulate reactant residence times at large active surface areas for selective catalysis.^{6–8} In this instance, flow rate is dictated by the kinetics of the reaction.⁹ The superior heat dissipation characteristics of microchannels can also be used for the restrained management of exothermic reactions and thus achieve further selectivity.^{10,11} Fluidic actuation can also be harnessed to achieve precise stoichiometric control of interacting species,^{12,13} or to allow concentration gradients to be constructed for stereoselection.¹⁴ Extension of this approach by

the incorporation of additional and integrated microchannels has been used to enable multi-step dipeptide synthesis.¹⁵ Another motivation includes the use of actuation methods such as capillary electrophoresis to exploit the differing mobilities of enzymes and substrates to affect the duration of biochemical interactions, while also removing products to allow successive conversions.¹⁶ It is evident that this approach to chemistry requires not only miniature geometries and fluidic actuation but also a careful consideration of channel design, material choice and actuation technique. We have used the term architecture controlled chemistry to encompass these features.

This paper describes the adoption of this approach for the amplification of DNA by the polymerase chain reaction (PCR). PCR is an enzymatically driven reaction that comprises a number of thermal cycles, each cycle typically comprising three temperatures. The target DNA molecule is first denatured into separate strands at an elevated temperature ($>90 \text{ }^\circ\text{C}$), then synthetic oligonucleotides (primers) undergo sequence specific annealing with the target strands at an appropriate temperature ($\sim 60 \text{ }^\circ\text{C}$). These primers then direct the enzymatic polymerization, or extension, of complementary DNA copies of the two strands at the optimum enzyme activity temperature, typically $74 \text{ }^\circ\text{C}$.¹⁷ Each cycle of PCR can therefore be regarded as a detection event followed by signal duplication, leading to the overall exponential synthesis of the desired product throughout the course of the reaction.¹⁸ This powerful amplification reaction is particularly advantageous for microsystems where detection capabilities are challenged by the minute volumes involved. The cycle of events during DNA amplification by PCR is depicted in Fig. 1.

Continuous flow PCR is based on a reaction conduit passing repetitively through the required temperature zones such that the shape of the conduit and the flow rate determines the temperature profile that the reactants experience.¹⁹ When operating in capillaries with micron dimensions, heat dissipation times become minimal, and heating and cooling is then largely restricted to flow rate.²⁰ Micromachined channels have been used to achieve total run times of the order of minutes,

† Electronic supplementary information (ESI) available: figures depicting a silicon MHD microreactor, finite element solution for velocity profile in the silicon microreactor annulus, and the effect of MHD actuation conditions on the PCR product previously generated by conventional amplification methods and on the PCR reagents prior to thermocycling by conventional methods. See <http://www.rsc.org/suppdata/lc/b2/b206756k/>

approaching the theoretical limit of PCR performance with zero ramping time.^{21,22}

2. Concept

Taking the micromachined continuous flow approach to DNA amplification we identified an alternative channel design to the conventional serpentine layout. The cyclical nature of the PCR chemistry suggests that a circular, or annular, channel could be used to conduct a thermal cycle every revolution. This arrangement is readily amenable to the implementation of a single detection element for the quantitation of product yield throughout the course of the reaction. On-line detection coupled with cycle number flexibility, again afforded by the circular geometry of the channel, can be used to avoid excessive thermal cycles and further allows the quantitation of original template copy number.²³ For efficient amplification, comparable to conventional thermocycling instruments, a cycle duration of three minutes or less is required. Given a channel diameter of 10 mm this demands fluid velocities of the order of $200 \mu\text{m s}^{-1}$. Moreover, the actuation of fluids in an annular channel poses a considerable challenge. Fluid circulation using a magnetohydrodynamic (MHD) micropump has previously been demonstrated and provides a means of addressing this.²⁴ This actuation mechanism operates without the use of a pressure drop to generate a flow that is effectively continuous, making it suitable for continuous flow reactions in a circular channel. MHD actuation is realised when an electric current is applied across a channel in a fashion that is perpendicular to a magnetic field originating from beneath the channel. This orthogonal arrangement generates a Lorentz force that is perpendicular to both electric and magnetic fields, and acts to induce fluid circulation.

3. Experimental

3.1 Fabrication

Annular MHD microreactors were realised by either bulk micromachining in silicon or by rapid prototyping using EPON SU-8, a thick film negative photoresist. Both annular microreactors have an adjoining microchannel for sample introduction and removal by centrifugation. SU-8 MHD microreactor prototypes with an annulus of internal radius 4.5 mm were fabricated using a $525 \mu\text{m}$ thick silicon substrate with $1 \mu\text{m}$ of SiO_2 grown in a wet furnace (Thermco 9000 Furnace). SU-8 was spin coated and developed using UV photolithography to realise $180 \mu\text{m}$ deep channels, with a width of $1000 \mu\text{m}$. The channel electrodes were defined using a standard sputtering method in conjunction with an experimental patterning technique involving stainless steel stencils. The circular geometry of the device demands two sets of complementary crescent stencils, and therefore two sputtering steps. In addition,

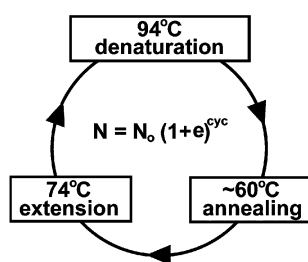


Fig. 1 Cycle of events during DNA amplification by PCR. Where N_0 is the original template copy number, e is the efficiency of fragment duplication, and N is the final copy number.

stainless steel channel inserts were required to ensure electrode separation at the base of the channel. Metallisation was achieved using a 30 min 1.5 kW RF etch to promote adhesion of electrodes (1000 nm Cu , 100 nm Pt) deposited on the vertical wall structures by sputtering (Nordiko Magnetron, MDX 2500-W) through the stencil and about the insert. These microreactors were enclosed using a $150 \mu\text{m}$ thick laminate. The SU-8 fabrication scheme and device are depicted in Figs. 2 and 3, respectively. The alternative device was fabricated using bulk micromachining, which involved anisotropic KOH etching an annulus into a $525 \mu\text{m}$ thick silicon substrate to a depth of $150 \mu\text{m}$, with an average width of $1160 \mu\text{m}$, and with an average internal radius of 4.42 mm . Following the growth of a $1 \mu\text{m}$ thick SiO_2 using a wet furnace (Thermco 9000 Furnace), the wafers were coated with metal (350 \AA Cr , 2000 \AA Au) using a Temascal Evaporator (BJD1800). Standard photolithographic methods were used with Eagle electrophoretic negative photoresist (ED2100) to pattern metal electrodes on the channel walls.²⁵ Finally, a UV-curable epoxy (Loctite 302) was used to

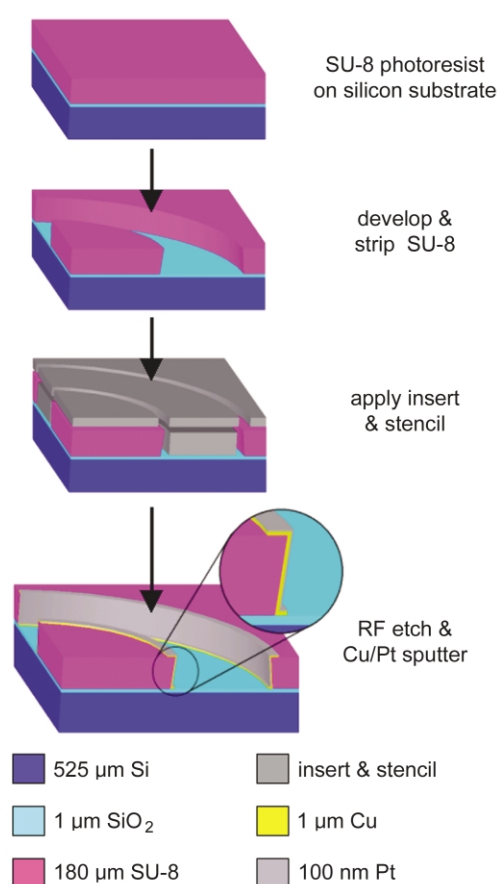


Fig. 2 Illustration of SU-8 microreactor fabrication path.

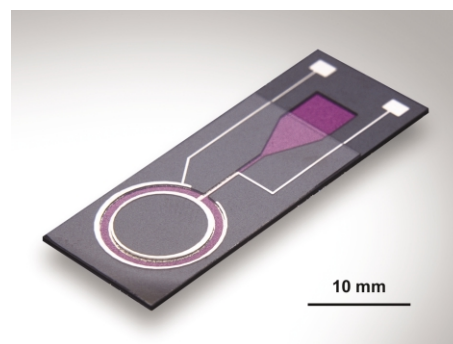


Fig. 3 MHD microreactor with an annular channel developed in SU-8 and with Cu/Pt electrodes patterned on the vertical wall structures.

enclose the microreactors with a 150 μm thick glass superstrate. The silicon device is shown in the supplementary material †(ESI), Fig. S1.

3.2 Flow modelling

A model was constructed to consider the effect of channel current and geometry during MHD actuation. By neglecting the effects of fluid motion on the magnetic and electric fields, the equations of incompressible MHD flow²⁶ may be reduced to the Navier–Stokes equation with a Lorentz force:

$$\rho \frac{D\mathbf{v}}{Dt} + \nabla p = \mathbf{j} \times \mathbf{B} + \eta \Delta \mathbf{v} \quad (1)$$

Here \mathbf{v} is the velocity of the fluid, \mathbf{B} is the magnetic field, \mathbf{j} is the current density and ρ , p and η are, respectively, the density, pressure and absolute viscosity of the fluid. This equation is to be solved for the fluid velocity, given the imposed current density \mathbf{j} and the magnetic field \mathbf{B} . The SU-8 microchannel geometry is cylindrically symmetric of width 1000 μm and depth, $h = 180 \mu\text{m}$. Eqn. (1) admits a cylindrically symmetric steady solution with radial velocity and axial velocity both zero, and azimuthal velocity v and pressure depending only on r and z (the radial and vertical coordinates). These assumptions simplify (1) to a Poisson equation for the steady azimuthal velocity, where B and I are the peak amplitudes of the AC electric and magnetic fields:

$$\Delta v - \frac{v}{r^2} = \frac{BI}{4\pi r h \eta}$$

This may be solved using a Fourier–Bessel expansion, or by straightforward numerical computation using a two-dimensional finite element package. The boundary conditions at the sides, bottom and top of the channel are determined by the standard no-slip condition ($v = 0$) for viscous fluid at a wall. Plotted in Fig. 4 is the nondimensional quantity

$$-v(r, z) \times \left(\frac{BI}{4\pi h \eta} \right)^{-1}$$

evaluated at each (r, z) point in the channel cross-section. This has a maximum near the inner wall, at half the depth, which corresponds to a dimensional velocity of magnitude

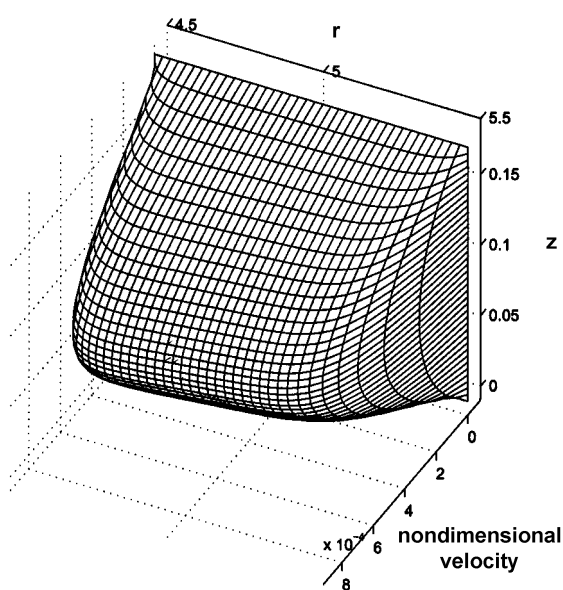


Fig. 4 Finite element solution for velocity profile in the SU-8 annulus. Depth is measured along the vertical z axis in mm. The microchannel width is 1 mm with channel radius in mm along the r axis.

$$v = 8.4 \times 10^{-4} \frac{BI}{4\pi h \eta} \quad (2)$$

The effective transport velocity is the average of the velocity over the cross-section of the SU-8 channel, and has a nondimensional value of 4.7×10^{-4} (*i.e.* 56% of the maximum given by (2) above). Note that the numerical value in eqn. (2) depends strongly on the channel geometry. Thus, for example, if the height of the SU-8 microchannel is approximately doubled to 375 μm , a new nondimensional multiplier of 3.4×10^{-3} (about 4 times larger than the 8.4×10^{-4} value in (2)) is calculated from the Poisson solver. For a given electrode voltage, it is observed that the value of the current I changes proportionally with channel height h and therefore the current density is maintained. Consequently the $BI/4\pi h \eta$ factor in (2) is unaltered, and the model predicts that the actuation velocity also scales with h^2 , for channel dimensions of the order considered here.

Calculation of the velocities in the silicon microreactor becomes more involved owing to the anisotropic etch that results in vertical walled regions (1278 μm wide), and 54° etch regions where the channels are wider at the top than the bottom (1045 μm and 830 μm , respectively), and still further regions where a combination of these cross-section geometries exist. Separate computation of the two cross-section extremes reveals only a 2% difference. This negligible difference arises from the dominating influence of the smallest dimension (height) and the high aspect ratio (~ 7). The nondimensional velocity profile in the 54° etch region can be found in the supplementary material †(ESI), Fig. S2. In this study an average nondimensional value of 5.9×10^{-4} was used to approximate the maximum velocity in the silicon microreactor, yielding an effective transport velocity with a nondimensional value of 3.3×10^{-4} .

3.3 Apparatus and operation

MHD actuation using a 1 kHz AC signal was implemented to avoid issues of net reactant migration leading to electrode and reactant degradation, and the accompanying electrolytic bubble generation, when operating in DC.²⁴ An elementary series circuit was used to synchronise sinusoidal electric and magnetic fields to generate a circulating Lorentz force. In this arrangement, the Lorentz force depends on the amplitude and oscillation state of the AC electric and magnetic fields. Thus during one period of oscillation a variation in the magnitude of the Lorentz force is seen, resulting in a pulsatile flow where the peak force generated is double that of the time-averaged force. However, operation at high frequencies (1 kHz) with a viscous fluid generates a flow that can be effectively regarded as continuous, reflecting the time-averaged force.²⁷

The experimental apparatus comprised an AC power source (HP 6813A) connected in series to the MHD chip and an electromagnet. The electromagnet was fabricated using 350 turns of copper wire about a ferrite tube. Multiple cover slips were used as spacers to provide 150 μm intervals for magnetic field measurements using a magnetic probe (GM05 Gaussmeter, Hirst). This data was used to calculate the average magnetic field experienced by the fluid in the microchannels of the SU-8 and the silicon MHD devices for a given electromagnetic current. Typical MHD actuation conditions used a 5 V_{RMS} signal applied to the circuit to provide a cross channel current of 90 mA and a magnetic field of 11 mT when using a 500 mM electrolyte at room temperature. The electrolyte comprised either KCl or PCR solutions (60 or 100 mM, *i.e.* 50 mM KCl with 10 or 50 mM Tris-HCl, respectively). Fluid velocities were determined by video microscopy of 6 μm diameter latex particles that serve as tracers for the observation of fluid movement. Temperature zones were realised using

contacting thermoelectric peltiers (ThermaTEC Series, MELCOR) driven by power sources (PSD3510A, WK) and surface temperatures were monitored using 0.005" gauge K-type thermocouples (Omega). The primer annealing and enzyme activity temperature was set to 72 °C, and the denaturation temperature was set to 92 °C. Using a viscometer (RV20, Haake) the absolute viscosity of a model PCR solution was found to approximate that of water in the measurement range of 25 °C–85 °C. The model solution contained 50 mM KCl, 10 mM Tris-HCl (pH 9.0), 0.1% Triton® X-100, 2 µM EDTA, 20 µM DTT, 1% (v/v) glycerol, 0.2 mM deoxynucleotides, 2 mM MgCl₂ and 40 µg mL⁻¹ BSA (polymerase substitute). When operating at an average channel temperature of 82 °C (validated by the associated cross channel current gain) the average absolute viscosity η was estimated to be 3.5×10^{-4} kg m⁻¹ s⁻¹ (or 0.35 cP). During thermocycling, average flow velocities were extrapolated from eqn. (2) using cross channel and electromagnet current measurements. The experimental set-up for thermocycling is depicted in Fig. 5.

3.4 PCR Engineering

To promote PCR-compatibility (biocompatibility) the devices were derivatised with a solution of 5 mg mL⁻¹ BSA (Sigma) and 5 mg mL⁻¹ crude oligonucleotides from herring sperm (Sigma-Aldrich) for 15 min at 4 °C. Biocompatibility experiments involved thermocycling device-contained PCR mixtures using a commercial PCR thermal block (Mastercycler gradient, Eppendorf), and exposure to actuation conditions for various periods both before and after PCR by conventional means.

The operational voltages required for high velocity MHD actuation can be associated with a pH change, and the PCR mixture was therefore tailored to provide improved buffering capacity. By increasing the buffer concentration (five-fold) the ionic content and cross channel current are also increased to enable actuation at voltages that are less deleterious to PCR performance. The amplification fragment was designed to contain the multi-drug resistance diagnostic region of the *rpoB* gene of *Mycobacterium tuberculosis*. PCR reactions were performed with reagents purchased from Promega Corporation: 50 mM KCl, 50 mM Tris-HCl (pH 9.0), 0.1% Triton® X-100, 2 µM EDTA, 20 µM DTT, 1% (w/v) glycerol, 0.2 mM deoxynucleotides, 2 mM MgCl₂, 1 µM primers (5'-CCGGCCGGTGGTCGCCGCGATCAAGGAGT-3', 5'-CACGCTCACGTGACAGACCGCCGGGC-CCC-3'), *Taq* DNA polymerase (0.1 U µL⁻¹), ~10⁶ template copies. Reaction volumes of ~6 µL were loaded into the microchannel by centrifugation and contained using ~100 nL of mineral oil to prevent evaporation. A two-step PCR chemistry was chosen and comprised denaturation at 92 °C, with primer annealing and enzyme activity at 72 °C, repeated for a total of 20 cycles. Reference and device-contained biocompatibility PCR reactions were performed in the commercial thermocycler. PCR products were separated on a 1.8% agarose (Sigma-Aldrich) gel

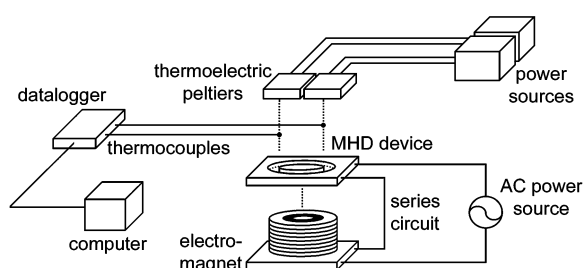


Fig. 5 Schematic drawing of the experimental set-up for continuous flow thermocycling by annular MHD actuation.

and visualised by UV transillumination using ethidium bromide (Sigma-Aldrich).

4. Results and discussion

4.1 Engineering

The MHD microreactors were fabricated with an adjoining channel for sample introduction and removal by centrifugation. This simple spin in/out method operates by first allowing the reagents to be dispensed into the trapezium-shaped inlet cavity by capillary action, followed by brief centrifugation steps (maximum of < 500g, 2000 rpm) to funnel the reagents into the annulus. This method is not associated with the formation of air pockets that would otherwise expand during thermocycling and impede fluid actuation. In addition, the mineral oil seal completely prevents evaporation to maintain reactant concentrations during thermocycling.

Thermal management problems are particularly pronounced when conducting continuous flow PCR with three disparate temperatures, and with a continuous and conductive medium. Here, inadequate thermal isolation retards temperature ramping efficacy leading to undesirable reaction kinetics. To alleviate this problem, primer design in terms of length and G:C composition was exploited to achieve annealing and elongation at 72 °C. Moreover, this 2-step PCR strategy effectively halves thermal ramping times leading to significantly reduced reaction times. These measures were introduced to provide a simple and robust continuous flow thermocycling chemistry for demonstration purposes. It is, however, recognised that later thermocycling systems require three temperature zones to provide the flexibility to accommodate the diversity of existing PCR chemistries.

4.2 Fabrication and biocompatibility issues

The encapsulation of microchannels is a recognised challenge. The use of a UV-curable glue was found to be a quick, easy and inexpensive method for the attachment of thin glass superstrates (cover slips) to a silicon substrate. With measured application the glue was not found to occlude the cavity and coat the electrodes. Instead, capillarity operates to evenly spread the uncured glue throughout the substrate/glass interface, and once the glue reaches the microchannel cavity these forces become negligible to prevent further spreading. The surface roughness of the SU-8 device does not favour this approach, but does make it suitable to promote the adhesion of a laminate. However, to prevent the collapse of the laminate suspended over the inlet cavity (distances > 2 mm) it was necessary to incorporate SU-8 pillars. The laminate was also found to be robust to PCR temperatures and thermocycling.

Rapid prototyping using SU-8 provides an easy and inexpensive route to fabricate deep structures with vertical walls.²⁸ A re-entrant wall profile (*i.e.* an overhang) occurs with deep structures (*e.g.* 180 µm) due to disparate temperature effects associated with lengthy UV exposure times. Metallisation of these structures is not trivial but was overcome with the proposed metallisation technique, where the high mobility of sputtered atoms can be used to attain coverage. Moreover, this method obviates the use of a resist and the associated processing steps. The Cu/Pt metallisation was, however, found to be vulnerable to temperature changes during thermocycling. The platinum is seen to detach from the copper layer beneath and buckle causing an apparent 'shrinkage' that exposes the copper. Fig. 6 reveals the effect of this stress on the metallisation. Following device-contained thermocycling a pH rise in the reaction mixture is also observed. This could be due to the creation of a Galvanic cell between the two metal layers in the

presence of an electrolyte that results in the oxidation of copper at the expense of platinum-catalysed hydrogen gas and hydroxide ion evolution from water. Electrochemical etching of the copper disrupts the metal-metal adhesion and makes this junction susceptible to thermocycling-induced damage that results from the metals' differing thermal expansion coefficients. Clearly these Cu/Pt metallised SU-8 devices are not sufficiently robust, but there is also an issue of biocompatibility. The buffer (even when enhanced to 50 mM-five-fold) cannot tolerate the electrochemical by-products and the reaction is consequently inhibited (this effect is not associated with SU-8 microchannels without Cu/Pt metallisation, data not shown). To overcome the problems associated with Cu/Pt metallisation, alternative and compatible metallisation partners, such as Cr/Au, can be used. Indeed, the Cr/Au metallised silicon microreactors were unaffected by thermocycling conditions and were found to be completely biocompatible once derivatised with BSA and DNA. Gel documentation of PCR products from a positive control, and following thermocycling in the SU-8 and silicon MHD microreactors is presented in Fig. 7. By conducting pre-PCR and post-PCR exposure tests it was further found

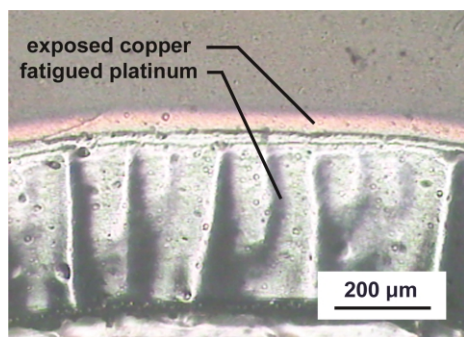


Fig. 6 Plan view image of the fatigued Pt/Cu metallisation on the internal microchannel wall reveals the effects of thermocycling.

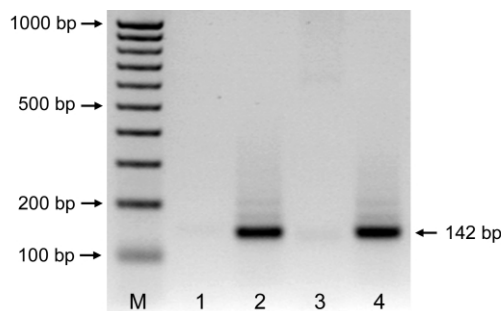


Fig. 7 Effect of microreactor materials derivatised with 5 mg mL⁻¹ BSA and 5 mg mL⁻¹ DNA on the amplification of a 142 bp product. From left to right, 100 bp increment ladder (M), negative control, *i.e.* PCR mixture without thermocycling treatment (lane 1), positive control, *i.e.* PCR conducted in 0.2 mL Eppendorf tube (lane 2), the effect of Cu/Pt metallised SU-8 (lane 3), and the effect of Cr/Au metallised silicon (lane 4).

that the MHD actuation conditions are not detrimental to either the PCR reagents or the PCR product. Experiments were conducted for periods of up to 3 h without influence on the final PCR product as determined by comparison with unexposed positive controls. Gel documentation of these findings can be found in the supplementary material †(ESI), Figs. S3 and S4.

4.3 MHD model and actuation

The cylindrical symmetry of the SU-8 device produces circular streamlines and therefore allows the model to be constructed using an exact reduction of the Navier-Stokes equation to the Poisson equation. The anisotropic etch used to fashion the silicon microchannel causes deviation from this cylindrical symmetry. However, the dimensions and symmetry present come close to producing circular streamlines and the model was therefore deemed appropriate to describe fluid circulation in the silicon MHD microreactor.

Both silicon and SU-8 microreactors were capable of providing Lorentz force conditions for MHD actuation of electrolytes comprising KCl or PCR reagents. Fig. 8 shows video microscopy frames of a latex particle moving at 342 μm s⁻¹ (92 s rev⁻¹) in the silicon MHD device. The velocities of particles transported by MHD-driven fluid streams were found to cluster around the average and beneath the peak velocity predicted by the relevant model. As shown in Table 1 this agreement was observed at numerous voltage inputs and for various electrolytes. This data does not reveal the disparate velocities seen throughout the channel's cross section, ranging from zero velocity (no-slip boundary condition) to those towards the peak velocity. This parabolic velocity profile is typical of liquids moving in the laminar flow regime and could have severe consequences for continuous flow chemistries. In this instance, the reactants residence time in a given temperature zone becomes highly variable, such that residence times may be too lengthy, with the result of polymerase inactivation in the denaturation zone, or too short, causing incomplete strand denaturation and polymerisation. This will have the effect of

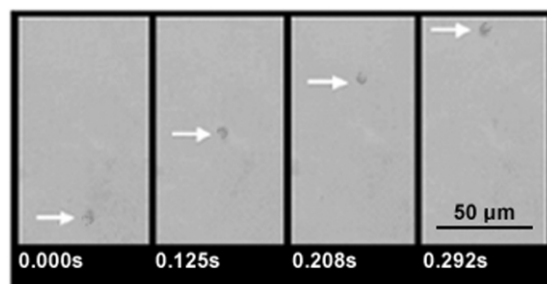


Fig. 8 Video microscopy frames of a particle moving at 342 μm s⁻¹ in a MHD-actuated stream of 500 mM KCl in the silicon device. Operational conditions comprised the application of a 7 V_{RMS} signal to the circuit to generate a channel current of 156 mA and an average channel magnetic field of 13.5 mT.

Table 1 The performance of the SU-8 and the silicon MHD micropumps. Experiments were conducted using KCl (aq) at room temperature (~20 °C) where the absolute viscosity η is 1×10^{-3} kg m⁻¹ s⁻¹. Observed velocity averages were calculated using data from 5 latex particles moving under the same actuation conditions.

Microreactor type	Electrolyte concentration/mM	Circuit voltage/V _{RMS}	Peak channel current/mA	Peak magnetic field/mT	Modelled velocity average/μm s ⁻¹	Observed velocity average/μm s ⁻¹
SU-8	100	6.00	55	7.4	85	86
Silicon	100	7.00	71	9.6	119	140
SU-8	500	5.00	89	10.8	200	240
Silicon	500	7.00	156	13.5	369	364

decreasing the overall reaction efficiency, with a requirement for further cycling. Given the dimensions involved and the increased diffusion rates at PCR temperatures, it is difficult to ascertain the significance of this problem. However, this effect is particularly pronounced for room temperature continuous flow chemistries that require rapid fluid actuation and therefore modifications to the microchannel surface or fluid composition should be made to impart dynamic conditions.^{21,29}

Application of an electrode voltage in excess of $4.9 V_{\text{RMS}}$ (circuit voltage of $7.0 V_{\text{RMS}}$) at 1 kHz was found to promote electrolysis that is associated with the formation of bubbles and a drop in the channel current. At this limiting voltage, calculated circulation times at PCR temperatures are of the order of 90 s rev^{-1} . However, when operating at PCR temperatures electrolysis occurs at considerably lower voltages ($0.6 V_{\text{RMS}}$), resulting in the occlusion of channels by bubbles and the formation of electrolysis by-products that could interfere with the PCR chemistry. At these temperatures reaction rates increase such that the 1 kHz frequency is not sufficient to reverse the accumulation of gaseous electrochemical by-products before bubble formation. Increasing the frequency was found to provide only mild relief at the expense of magnetic field strength and a phase shift that further reduces the Lorentz force, and therefore does not represent a solution. Similarly, an increase in the liquid's ionic character (limited by the reaction's 50 mM Tris-HCl tolerance) confers only minimal channel current gains at the same driving voltage. Circuit revisions were considered to amplify the magnetic field while maintaining the electrode voltage below $0.6 V_{\text{RMS}}$. However, simple calculation reveals that this approach can only achieve velocities of $\sim 60 \mu\text{m s}^{-1}$ (9 min rev^{-1}). This modest circulation speed results in lengthy temperature transitions such that template strands will be recombined before primers anneal and the reaction will therefore be inhibited.

To combat these issues, future designs consider the fabrication of silicon or glass microreactors with deeper channels to exploit the scaling principles of the MHD phenomenon. This could be achieved using methods such as deep reactive ion etching (DRIE) or advanced silicon etching (ASE). Other possibilities include the use of ceramic tapes to realise channels with a depth in excess of $500 \mu\text{m}$.³⁰ The value of this approach is realised when considering that the model predicts, for example, an approximate four-fold increase in fluid velocity with a doubling of the channel depth. The electrode separation distance can also be increased by the use of a vertical etch method but also by more careful metallisation mask design. In this study a generous Cr/Au metallisation mask was used that resulted in a minimum electrode separation distance of $600 \mu\text{m}$, leading to a lowering of the electrolysis threshold. With the benefit of etch simulation software such as SIMODE, the electrodes can be more accurately patterned on the silicon channel walls to give an increase in the electrode separation distance. However, increasing the channel dimensions represents a step away from the advantages gained with miniaturisation. Instead, a more powerful magnet is preferred. The device could be clamped with a C magnet to concentrate the magnetic flux and attain significant gains in magnetic field strength. For example, a magnetic field strength of 200 mT would enable flow velocities of $750 \mu\text{m s}^{-1}$ ($\sim 40 \text{ s rev}^{-1}$). This approach demands the incorporation of thermistor elements within the microchannel for localised thermal management.

5. Conclusions

This paper describes first generation microreactor prototypes for continuous flow thermocycling chemistries. A central design feature was the use of a microfabricated annulus to accommodate the nature of the chemical process. The circula-

tion of fluids was made possible using MHD actuation and this pumping mechanism was accurately modelled with respect to the system's geometry and channel current density. The described MHD microreactors were however confounded by electrolysis at elevated temperatures, but an understanding of the limits of this technology has provided design criteria for the next generation of microreactors. Alternatively, MHD actuation would be favoured for applications involving strong electrolytes or even ionic liquids, where pumping methods such as electro-osmotic flow are compromised.³¹ Annular MHD reactors are but one example of systems for conducting architecture controlled chemistry. With appropriate choice of channel arrangement, actuation method and materials other architecture controlled chemistries are possible. Further elaboration to more exotic systems with additional interconnecting reservoirs, capillaries and valving techniques will accommodate more sophisticated chemistries that involve precision timing of the encounter of chemical species throughout the course of a chemical pathway.

Acknowledgements

The authors gratefully acknowledge Jan Krüger, Joe O'Brien, Pdraig Hughes and Ye Shu-Ren (NMRC) for assistance with fabrication, Damien Arrigan (NMRC) for electrochemistry input, Mark Hickey (Dept. Applied Mathematics, UCC) for model validation and Lucía García (Pharma Gen S.A.) for the provision of PCR template. The research was partly supported by the Enterprise Ireland International Collaboration Fund, and by the EU under the DISSARM QLK-CT-2000-00765 project.

References

- 1 W. Ehrfeld, K. Golbig, V. Hessel, H. Löwe and T. Richter, *Ind. Eng. Chem. Res.*, 1999, **38**, 1075.
- 2 C. Erbacher, F. G. Bessoth, M. Busch, E. Verpoorte and A. Manz, *Mikrochim. Acta*, 1999, **131**, 19.
- 3 R. D. Chambers and R. C. H. Spink, *Chem. Commun.*, 1999, 883.
- 4 J. R. Burns and C. Ramshaw, *Trans Inst. Chem. Eng.*, 1999, **77**, 206.
- 5 J. P. Brody, P. Yager, R. E. Goldstein and R. H. Austin, *Biophys. J.*, 1996, **71**, 3430.
- 6 G. Weißmeier and D. Hönicke, *J. Micromech. Microeng.*, 1996, **6**, 285.
- 7 A. J. Franz, K. F. Jensen and M. A. Schmidt, in *Microreaction Technology: Industrial Prospects*, ed. W. Ehrfeld, Springer, Berlin, 2000, pp. 267–277.
- 8 J. J. Lerou, M. P. Harold, J. Ryley, J. Ashmead, T. C. O'Brien, M. Johnson, J. Perrotto, C. T. Blaisdell, T. A. Rensi and J. Nyquist, in *Microsystem Technology for Chemical and Biological Microreactors: Papers of the Workshop on Microsystem Technology*, Mainz, DECHEMA, Frankfurt, 1995, pp. 51–69.
- 9 M. W. Losey, M. A. Schmidt and K. F. Jensen, in *Microreaction Technology: Industrial Prospects*, ed. W. Ehrfeld, Springer, Berlin, 2000, pp. 277–286.
- 10 T. Richter, W. Ehrfeld, K. Gebauer, K. Golbig, V. Hessel, H. Löwe and A. Wolf, in *Process Miniaturization: Second International Conference on Microreaction Technology*, New Orleans, AIChE, LA, 1998, pp. 146–151.
- 11 R. Srinivasan, I-M. Hsing, P. E. Berger and K. F. Jensen, *AIChE J.*, 1997, **43**, 3059.
- 12 A. G. Hadd, D. E. Raymond, J. W. Halliwell, S. C. Jacobson and J. M. Ramsey, *Anal. Chem.*, 1997, **69**, 3407.
- 13 V. Skelton, G. M. Greenway, S. J. Haswell, P. Styring, D. O. Morgan, B. H. Warrington and S. Y. F. Wong, *Analyst*, 2001, **126**, 7.
- 14 V. Skelton, G. M. Greenway, S. J. Haswell, P. Styring, D. O. Morgan, B. H. Warrington and S. Y. F. Wong, *Analyst*, 2001, **126**, 11.
- 15 P. Watts, C. Wiles, S. J. Haswell, E. Pombo-Villar and P. Styring, *Chem. Commun.*, 2001, 990.

- 16 L. Z. Avila and G. M. Whitesides, *J. Org. Chem.*, 1993, **58**, 5508.
- 17 R. K. Saiki, S. Scharf, F. Faloona, K. B. Mullis, G. T. Horn, H. A. Erlich and N. Arnheim, *Science*, 1985, **230**, 1350.
- 18 T. M. Woudenberg, E. S. Winn-Deen and M. Albin, in *Proceedings μ TAS-96*, Basel, Switzerland, 1996, pp. 55–59.
- 19 M. D. Larzul, US patent 5176203, 1993. ***** *The seminal idea for conducting continuous flow biological processes in a tubing-type reactor.*
- 20 H. Nakano, K. Matsuda, M. Yohda, T. Nagamune, I. Endo and T. Yamane, *Biosci., Biotechnol., Biochem.*, 1994, **58**, 349. ***** *The first demonstration of continuous flow PCR in a tubing-type reactor.*
- 21 M. U. Kopp, A. J. de Mello and A. Manz, *Science*, 1998, **280**, 1046. ****** *This paper was the first to adopt microfabrication technology for continuous flow PCR. The scales involved enable superior heat transfer for rapid thermocycling.*
- 22 I. Schneegaß, R. Bräutigam and J. M. Köhler, *Lab Chip*, 2001, **1**, 42.
- 23 T. Wittwer, M. G. Herrmann, A. A. Moss and R. P. Rasmussen, *BioTechniques*, 1997, **22**, 130.
- 24 A. V. Lemoff and A. P. Lee, *Sens. Actuators, B*, 2000, **63**, 178. ****** *The first demonstration of magnetohydrodynamic actuation for fluid circulation in a microfabricated system.*
- 25 J. O'Brien, P. J. Hughes, M. Brunet, B. O'Neill, J. Alderman, B. Lane, A. O'Riordan and C. O'Driscoll, *J. Micromech. Microeng.*, 2001, **11**, 353.
- 26 J. A. Shercliff, *A Textbook of Magnetohydrodynamics*, Pergamon Press, 1965.
- 27 A. V. Lemoff and A. P. Lee, *Proceedings μ TAS-2000*, Enschede, The Netherlands, 2000, pp. 571–574.
- 28 H. Lorenz, M. Despont, N. Fahrmi, J. Brugger, P. Renaud and P. Vettiger, *Sens. Actuators, A*, 1998, **64**, 33.
- 29 N. Chiem and D. J. Harrison, *Anal. Chem.*, 1997, **69**, 373.
- 30 J. Zhong, M. Yi and H. H. Bau, *Sens. Actuators, A*, 2002, **96**, 59.
- 31 G. Kemp, *Biotech. Appl. Biochem.*, 1998, **27**, 9.